Direct and inverse scattering from dispersive media

Fuks, Peter; Karlsson, Anders; Larson, Gunnar

1993

CODEN:LUTEDX/(TEAT-7025)/1-21/(1993)

Direct and inverse scattering from dispersive media

Peter Fuks, Anders Karlsson and Gunnar Larson

Department of Electroscience
Electromagnetic Theory
Lund Institute of Technology
Sweden

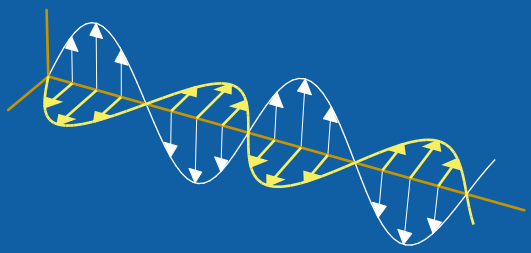

Peter Fuks

Department of Electromagnetic Theory
Royal Institute of Technology
SE-100 44 Stockholm
Sweden

Anders Karlsson

Department of Electromagnetic Theory
Lund Institute of Technology
P.O. Box 118
SE-221 00 Lund
Sweden

Gunnar Larson

Department of Electromagnetic Theory
Royal Institute of Technology
SE-100 44 Stockholm
Sweden

Editor: Gerhard Kristensson

Abstract

Direct and inverse scattering from dispersive media are studied in the time domain. The media are one-dimensional and homogeneous but can be impedance mismatched to the surrounding media. A time domain method is introduced where the reflection and transmission kernels are obtained from Volterra equations of the second kind. Numerical examples are given based upon both synthetic and measured data for the inverse problem.

1 Introduction

The dispersion relations for polar liquids have been extensively examined by time domain spectroscopy. The inverse scattering method presented in this paper has been developed with these applications in mind, eventhough it is a general method for dispersive media. The dispersive effects of a polar liquid are due to the frequency dependence of the complex permittivity. The majority of earlier results on the determination of the complex permittivity are based upon reflection measurements, *cf.* [3]– [5], but also transmission measurements have been used, *cf.* [6]. The construction of the complex permittivity from the measured data are mostly done in the frequency domain. The reflected or transmitted signal is then Fourier transformed and by dividing by the Fourier transform of the incident signal the reflection or transmission coefficient is formed. These coefficients are nonlinear functions of the complex permittivity and the explicit expressions are well-known. These nonlinear equations are to be solved for the complex permittivity. The solution to the equations are non-unique and a major problem in a frequency domain approach is to pick the right solution. Different techniques have been used to get the correct solution, *cf. e.g.*, [4] and [5]. The time-domain methods that have been used are only approximate, *cf.* [3].

In the present paper a time domain technique is presented for the inverse problem of finding the dispersion relation from a time domain spectroscopy experiment. The direct scattering problem is analyzed by the same technique. The major advantages of this time domain method over frequency domain methods are that the inverse problem is reduced to a uniquely solvable problem and that the solution is also guaranteed to be causal. In the time domain the dispersive medium is characterized by a susceptibility kernel. This kernel is the Fourier transform of the susceptibility and acts as a memory function for the polarization. The inverse problem is to obtain this susceptibility kernel from reflected or transmitted data. The corresponding direct problem is to obtain the reflected or transmitted field given the susceptibility kernel and the incident field.

In the present method the inverse method is solved in two steps. In the first step the reflection or transmission kernels are obtained by deconvolution from measured reflected or transmitted fields. The kernels are the impulse response of the medium. It is seen that the impulse response is related to the susceptibility kernel by Volterra equations of the second kind. These Volterra equations are well-posed and are straightforward to solve numerically. Given the exact reflection or transmission

kernels the susceptibility kernel can be obtained with any accuracy. There are other time-domain methods for solving the inverse problem, *cf.* [1] and [10]. Those methods are more general in that they can be generalized to inhomogeneous media. However, for homogeneous media, they lead to much slower algorithms than the ones obtained from the method presented in this paper.

In Section 2 the constitutive relation for a dispersive dielctric, the wave equation and the boundary conditions are presented. In Section 3 reflection and transmission operators are introduced and relations between these operators are derived. In Section 4 the scattering operators are represented by reflection and transmission kernels and it is seen that the operator relations lead to Volterra equations of the second kind. The relation between the susceptibility kernel and the transmission and reflection kernels are derived in Section 5. The slab is impedance mismatched to the surrounding media which implies that the scattering kernels will be discontinuous. The values and locations of these discontinuities are given in Section 6. The algorithms for the direct and inverse problem are presented in Section 7 and 8, respectively. The theory have been successfully tested with measured data. In the numerical section one such test is presented. There are also two examples where the theory is tested with synthetic data.

2 Basic relations

A dispersive medium is characterized by the constitutive relations between the electric field $\boldsymbol{E}$, the displacement field $\boldsymbol{D}$, the magnetic induction $\boldsymbol{B}$, and the magnetic field $\boldsymbol{H}$. In the simplest case of a non-magnetic medium the constitutive relations in the time domain read, *cf.* [8] and [2]

$$\begin{aligned} \boldsymbol{D}(\boldsymbol{r},t) &= \varepsilon_0\varepsilon_r(\boldsymbol{r})\boldsymbol{E}(\boldsymbol{r},t) + \varepsilon_0 \textstyle\int_{-\infty}^{t} \chi(\boldsymbol{r},t-t')\boldsymbol{E}(\boldsymbol{r},t')\,dt' \\ \boldsymbol{B}(\boldsymbol{r},t) &= \mu_0\boldsymbol{H}(\boldsymbol{r},t). \end{aligned} \tag{2.1}$$

Here ε_0 and μ_0 are the permittivity and permeability of vacuum, respectively, ε_r is the relative permittivity and $\chi(\boldsymbol{r},t)$ is the susceptibility kernel. The relative permittivity reflects the instantaneous, or optical, respons of the medium. Instantaneous then means that the time for the respons is much shorter than the typical time scale for the variation of the electric field. It is common that media are modelled with a relative permittivity greater than one for electric fields in the microwave regime. The susceptibility kernel χ is a memory function which determines the dispersion of the medium. There are certain restrictions the susceptibility kernel has to meet in order for the medium to satisfy energy conservations. These restrictions are given in [9]. In the numerical section some specific models for the susceptibility kernel will be discussed.

In the present paper only homogeneous media are considered, i.e. ε_r is a constant and $\chi(t)$ is space independent. The dispersive medium occupies the region $0 < z < L$ and outside this slab there is a non-dispersive dielectric medium with relative permittivity ε_{r1}. A transient wave $\boldsymbol{E}(z,t) = E(z,t)\hat{x}$ impinges from the region

$z < 0$ on the slab at time $t = 0$. The constitutive relation in Eq. (2.1) then simplify to

$$D(z,t) = \varepsilon_0 \varepsilon_r E(z,t) + \varepsilon_0 [\chi(\cdot) * E(z,\cdot)](t).$$

The short hand notation for the convolution

$$[f * g](t) = \int_0^t f(t-t')g(t')\,dt'$$

will be used throughout the paper. The magnetic field will be directed in the $y-$direction, $\boldsymbol{H}(z,t) = H(z,t)\hat{y}$, and thus the Maxwell equations read

$$\begin{aligned} \partial_z E(z,t) &= -\mu_0 \partial_t H(z,t) \\ \partial_z H(z,t) &= -\varepsilon_0 \left(\varepsilon_r \partial_t E(z,t) + [\chi(\cdot) * \partial_t E(z,\cdot)](t)\right). \end{aligned} \tag{2.2}$$

The corresponding wave equation for $E(z,t)$ is

$$(\partial_z{}^2 - c^{-2}\partial_t{}^2)E(z,t) - c_0^{-2}[\chi(\cdot) * \partial_t{}^2 E(z,\cdot)](t) = 0.$$

where $c = (\mu_0 \varepsilon_0 \varepsilon_r)^{1/2}$ is the wave front speed in the slab and $c_0 = (\mu_0 \varepsilon_0)^{1/2}$ is the speed of light in vacuum. A wave splitting is now done with respect to the principal part, $\partial_z^2 - c^{-2}\partial_t^2$, of the wave equation. The following change of basis is introduced

$$E^{\pm}(z,t) = \frac{1}{2}\left\{E(z,t) \pm ZH(z,t)\right\} = \frac{1}{2}\left\{E(z,t) \mp c\int_0^t \partial_z E(z,t')\,dt'\right\},$$

where Z is the wave impedance

$$Z = \sqrt{\frac{\mu_0}{\varepsilon_0 \varepsilon_r}}.$$

The wave impedance outside the slab is denoted Z_1. In the non-dispersive regions $z < 0$ and $z > L$ the split fields E^+ and E^- are left (negative $z-$direction) and right (positive $z-$direction) moving waves, respectively. It is convenient to introduce the incident, reflected, and transmitted fields as:

$$\begin{aligned} E^i(z,t) = E^+(z,t) = E^+(0^-, t + z/c_1) &= \text{The incident field for } z < 0. \\ E^r(z,t) = E^-(z,t) = E^-(0^-, t - z/c_1) &= \text{The reflected field for } z < 0. \\ E^t(z,t) = E^+(z,t) = E^+(L^+, t - (z-L)/c_1) &= \text{The transmitted field for } z > L. \end{aligned}$$

where $c_1 = (\mu_0 \varepsilon_0 \varepsilon_{r1})^{-1/2}$ is the wave front speed outside the slab.

The boundary conditions at $z = 0$ and $z = L$ are that both the electric and magnetic fields are continuous

$$E^r(0^-,t) = r_0 E^i(0^-,t) + t_1 E^-(0^+,t) \tag{2.3}$$

$$E^+(0^+,t) = t_0 E^i(0^-,t) + r_1 E^-(0^+,t) \tag{2.4}$$

$$E^-(L^-,t) = r_1 E^+(L^-,t) \tag{2.5}$$

$$E^t(L^+,t) = t_1 E^+(L^-,t). \tag{2.6}$$

The reflection and transmission coefficients are defined as

$$\begin{aligned} r_0 = -r_1 &= \tfrac{Z - Z_1}{Z + Z_1} \\ t_0 &= \tfrac{2Z}{Z + Z_1} \\ t_1 &= \tfrac{2Z_1}{Z + Z_1}. \end{aligned}$$

3 Scattering operators

The strategy to solve the scattering problem is to split it into three parts. In the first part the scattering operators for an impedance matched slab are determined. The half-spaces $z < 0$ and $z > L$ are then impedance matched to the slab, i.e., the relative permittivity equals ε_r everywhere. The second part concerns the scattering operators for a slab with an impedance mismatched backwall $z = L$, i.e. where the half-space $z > L$ has the permittivity ε_{r1}. These operators are related to the operators for the impedance matched slab through the boundary conditions at $z = L$. In the last part the scattering operators for the entire slab, i.e. a slab with an impedance mismatched frontwall and backwall, are introduced. By utilizing the boundary conditions at $z = 0$ these operators are related to the operators for the slab with an impedance mismatched backwall. This technique of finding relations between scattering operators has some similarities with the Redheffer star product method, *cf.* [12].

The following scattering operators will be used in the analysis:

$$E^r(0,t) = \mathcal{R}E^i(0,t) \tag{3.1}$$
$$E^t(L,t) = \mathcal{T}E^i(0,t) \tag{3.2}$$
$$E^-(0^+,t) = \mathcal{G}_b^- E^+(0^+,t) \tag{3.3}$$
$$E^t(L,t) = \mathcal{G}_b^+ E^+(0^+,t) \tag{3.4}$$
$$E^-(0^+,t) = \mathcal{G}^- E^+(0^+,t) + \mathcal{F}^- E^-(L^-,t) \tag{3.5}$$
$$E^+(L^-,t) = \mathcal{G}^+ E^+(0^+,t) + \mathcal{F}^+ E^-(L^-,t) \tag{3.6}$$

The interpretation of these operators are:

$\mathcal{R}$ = The reflection operator for the entire slab.

$\mathcal{T}$ = The transmission operator for the entire slab.

$\mathcal{G}_b^-$ = The reflection operator for the slab with a matched frontwall $z = 0$ but a mismatched backwall $z = L$.

$\mathcal{G}_b^+$ = The transmission operator for the slab with a matched frontwall and mismatched backwall.

$\mathcal{G}^-$ = The reflection operator for the slab with matched front- and backwall.

$\mathcal{G}^+$ = The transmission operator for the slab with matched front- and backwall.

$\mathcal{F}^+$ = The reflection operator for transmission from $z = L$ to $z = 0$ for the impedance matched slab.

$\mathcal{F}^-$ = The transmission operator for transmission from $z = L$ to $z = 0$ for the impedance matched slab.

Since the slab is isotropic and thus reciprocal it follows that

$$\mathcal{F}^- = \mathcal{G}^+ \tag{3.7}$$
$$\mathcal{F}^+ = \mathcal{G}^-. \tag{3.8}$$

It is also convenient to introduce $\mathcal{W}$ as the inverse operator of $\mathcal{G}^+$

$$\mathcal{W}\mathcal{G}^+ = \mathcal{I} = \text{the identity operator.} \tag{3.9}$$

This means that

$$E^+(0^+,t) = \mathcal{W}\left(E^+(L^-,t) - \mathcal{G}^- E^-(L^-,t)\right). \tag{3.10}$$

A number of useful relations between the scattering operators can be found by utilizing the boundary conditions. The relations obtained in this section are in the next section seen to result in Volterra equations for the scattering kernels. From Eqs. (3.3), (3.5), and (3.7) it is seen that

$$\mathcal{G}_b^- E^+(0^+,t) = \mathcal{G}^- E^+(0^+,t) + \mathcal{G}^+ E^-(L^-,t). \tag{3.11}$$

In this relation $E^+(0^+,t)$ can be expressed in terms of $E^\pm(L^-,t)$ from Eqs. (3.10), (3.3), (3.5), and (3.7) and thus

$$\begin{aligned} &\mathcal{G}_b^- \mathcal{W}\left(E^+(L^-,t) - \mathcal{G}^- E^-(L^-,t)\right) = \\ &= \mathcal{G}^- \mathcal{W}\left(E^+(L^-,t) - \mathcal{G}^- E^-(L^-,t)\right) + \mathcal{G}^+ E^-(L^-,t). \end{aligned} \tag{3.12}$$

By using the boundary condition in Eq. (2.5) the following operator identity is obtained from Eq. (3.12)

$$\mathcal{G}_b^-(\mathcal{W} - r_1\mathcal{G}^-\mathcal{W}) = \mathcal{G}^-(\mathcal{W} - r_1\mathcal{G}^-\mathcal{W}) + r_1\mathcal{G}^+.$$

By applying the operator $\mathcal{G}^+$ and using the identity in Eq. (3.9), the final relation between $\mathcal{G}_b^-$ and $\mathcal{G}^\pm$ follows

$$\mathcal{G}_b^- - r_1\mathcal{G}_b^-\mathcal{G}^- = \mathcal{G}^- - r_1(\mathcal{G}^-\mathcal{G}^- - \mathcal{G}^+\mathcal{G}^+). \tag{3.13}$$

The relation between $\mathcal{G}_b^+$ and $\mathcal{G}^\pm$ is obtained in a similar fashion. From the operator relation in Eqs. (3.4), (3.6) and the boundary condition Eq. (2.6) it is seen that

$$\mathcal{G}_b^+ E^+(0^+,t) = t_1(\mathcal{G}^+ E^+(0^+,t) + \mathcal{G}^- E^-(L^-,t)).$$

Utilizing Eq. (3.10) and the boundary condition Eq. (2.5) to eliminate $E^+(0^+,t)$ from this relation implies

$$\mathcal{G}_b^+(\mathcal{W} - r_1\mathcal{W}\mathcal{G}^-) = t_1\mathcal{G}^+\mathcal{W}.$$

The operator $\mathcal{W}$ is eliminated by operating with $\mathcal{G}^+$, thus

$$\mathcal{G}_b^+ - t_1\mathcal{G}^+ - r_1\mathcal{G}_b^+\mathcal{G}^- = 0. \tag{3.14}$$

The final relations to be obtained are the ones between $\mathcal{R}$, $\mathcal{T}$, and $\mathcal{G}_b^\pm$. By using the relations in Eqs. (3.1) and (3.3), $E^\pm(0^+,t)$ and $E^r(0,t)$ can be eliminated from the boundary conditions (2.3) and (2.4). The resulting relation reads

$$\mathcal{R} - r_0\mathcal{I} - \mathcal{G}_b^- - r_1\mathcal{G}_b^-\mathcal{R} = 0. \tag{3.15}$$

The transmission operator $\mathcal{T}$ can be expressed in terms of the operators $\mathcal{G}_b^+$ and $\mathcal{R}$ by combining Eqs. (3.2) and (3.4) and utilizing the boundary conditions, Eqs. (2.3) and (2.4), giving

$$t_1\mathcal{T} - \mathcal{G}_b^+ + r_0\mathcal{G}_b^+\mathcal{R} = 0. \tag{3.16}$$

An alternative relation is found from Eqs. (2.4) and (3.3) which imply

$$E^+(0^+,t) = t_0E^i(0,t) + r_1\mathcal{G}_b^- E^+(0^+,t).$$

By applying the operator product $\mathcal{G}_b^+\mathcal{T}$ to this relation and assuming that the operators commute the relation is expressed solely in terms of the field $E^t(L,t)$. The relation

$$\mathcal{T} - t_0\mathcal{G}_b^+ - r_1\mathcal{G}_b^-\mathcal{T} = 0 \tag{3.17}$$

follows.

4 The scattering kernels

From arguments based upon invariance under time translation and causality it is shown that the explicit expressions for the operators $\mathcal{G}^-$ and $\mathcal{G}^+$ read, *cf.* [10],

$$\mathcal{G}^-E^+(0^+,t) = [R(\cdot) * E^+(0^+,\cdot)](t) \tag{4.1}$$

$$\mathcal{G}^+E^+(0^+,t) = dE^+(0^+,t-\frac{\tau}{2}) + \int_0^{t-\tau/2} T(t-t'-\tau/2)E^+(0^+,t')\,dt', \tag{4.2}$$

where

$$\tau = \frac{2L}{c}$$

is the roundtrip travel time and

$$d = \exp\left(-\frac{\tau\chi(0)}{4\varepsilon_r}\right)$$

is the attenuation of the wavefront for the transmitted field. The kernels R and T are the reflection kernel and transmission kernel, respectively, for a dispersive slab which is impedance matched to the half-spaces $z < 0$ and $z > L$. It is convenient to introduce an operator for time translation defined as

$$u(t-t_0) = \mathcal{S}(t_0)u(t), \tag{4.3}$$

where obviously

$$\mathcal{S}(t_1)\mathcal{S}(t_2) = \mathcal{S}(t_1+t_2).$$

Thus Eq. (4.2) reads

$$\mathcal{G}^+E^+(0^+,t) = \mathcal{S}(\tau/2)\left(dE^+(0^+,t) + [T(\cdot) * E^+(0^+,\cdot)](t)\right) \tag{4.4}$$

The representations of the operators in Eqs. (3.3)–(3.6) now follows from Eqs. (4.1) and (4.2) and the operator relations in the previous section.

When the representations in Eqs. (4.1) and (4.2) are inserted into Eq. (3.13) it is seen that the operator $\mathcal{G}_b^-$ has the representation

$$\mathcal{G}_b^- E^+(0^+,t) = r_1 d^2 \mathcal{S}(\tau) E^+(0^+,t) + [R_b(\cdot) * E^+(0^+,\cdot)](t), \tag{4.5}$$

and that the kernel R_b satisfies the Volterra equation of the second kind

$$\begin{aligned} &R_b(t) - R(t) + r_1\left([R*R](t) - [R_b*R](t)\right) - \\ &-\mathcal{S}(\tau)\left(r_1^2 d^2 R(t) + 2r_1 dT(t) + r_1[T*T](t)\right) = 0. \end{aligned} \tag{4.6}$$

The representation of the operator $\mathcal{G}_b^+$ is found by combining Eqs. (4.1) and (4.2) with the relation in Eq. (3.14). It turns out that

$$\mathcal{G}_b^+ E^+(0^+,t) = \mathcal{S}(\tau/2)\left(t_1 dE^+(0^+,t) + [T_b(\cdot) * E^+(0^+,\cdot)](t)\right), \tag{4.7}$$

where the kernel T_b satisfies the Volterra equation

$$T_b(t) = t_1 T(t) + t_1 r_1 dR(t) + r_1[T_b * R](t). \tag{4.8}$$

It remains to find the representation of the scattering operators for the entire slab, i.e. $\mathcal{R}$ and $\mathcal{T}$. The representation of the reflection operator $\mathcal{R}$ is a consequence of the operator relation in Eq. (3.15) and the representation of $\mathcal{G}_b^-$ given by Eq. (4.5):

$$\mathcal{R}E^i(0,t) = \sum_{j=0}^{\infty} a_j \mathcal{S}(j\tau) E^i(0,t) + [R_f(\cdot) * E^i(0,\cdot)](t), \tag{4.9}$$

where

$$\begin{aligned} a_0 &= r_0 \\ a_1 &= t_0 t_1 r_1 d^2 \\ a_j &= -r_0 r_1 d^2 a_{j-1}, \qquad j = 2,3,4,... \end{aligned}$$

Equivalently the representation of $\mathcal{R}$ can be written

$$\begin{aligned} \mathcal{R}E^i(0,t) = r_0 E^i(0,t) + t_0 t_1 r_1 d^2 \mathcal{S}(\tau)(1 + r_0 r_1 d^2 \mathcal{S}(\tau))^{-1} E^i(0,t) + \\ + [R_f(\cdot) * E^i(0,\cdot)](t) \end{aligned} \tag{4.10}$$

It is seen that the reflection kernel R_f is a piecewise continuous function of time which is related to the kernel R_b by the Volterra equation

$$R_f - R_b + r_0[R_f * R_b] + r_0 r_1 d^2 \mathcal{S}(\tau) R_f + r_0 \sum_{j=0}^{\infty} a_j \mathcal{S}(j\tau) R_b = 0. \tag{4.11}$$

The representation of the transmission operator $\mathcal{T}$ is found from Eq. (4.7) and Eq. (3.16) or Eq. (3.17)

$$\mathcal{T}E^i(0,t) = \mathcal{S}(\tau/2)\left(\sum_{j=0}^{\infty} b_j \mathcal{S}(j\tau) E^i(0,t) + [T_f(\cdot) * E^i(0,\cdot)](t)\right). \tag{4.12}$$

The coefficients b_j are

$$\begin{aligned} b_0 &= t_0 t_1 d \\ b_j &= -r_0 r_1 d^2 b_{j-1}, \qquad j = 1, 2, 3... \end{aligned}$$

In a closed form the representation reads

$$\mathcal{T} E^i(0,t) = \mathcal{S}(\tau/2) \left(t_0 t_1 d (1 + r_0 r_1 d^2 \mathcal{S}(\tau))^{-1} E^i(0,t) + [T_f(\cdot) * E^i(0,\cdot)](t) \right). \quad (4.13)$$

The transmission kernel T_f is a piecewise continuous function of time that satisfies the Volterra equation

$$T_f - t_0 T_b + r_0 [T_f * R_b] + r_0 r_1 d^2 \mathcal{S}(\tau) T_f(t) + r_0 \sum_{j=0}^{\infty} b_j \mathcal{S}(j\tau) R_b(t) = 0, \quad (4.14)$$

as seen from the relation in Eq. (3.17). An alternative representation of T_f is derived from Eq. (3.16)

$$T_f = {t_1}^{-1} T_b + r_1 d R_f + r_1 {t_1}^{-1} [T_b * R_f] + r_1 {t_1}^{-1} \sum_{j=0}^{\infty} a_j \mathcal{S}(j\tau) T_b. \quad (4.15)$$

In this last explicit expression it is necessary to know R_f as well as R_b and T_b in order to calculate T_f, whereas in the Volterra equation (4.14) only R_b and T_b were needed.

5 The kernels R and T

As mentioned in the previous section the kernels R and T are the reflection and transmission kernels for a dispersive slab with permittivity ε_r imbedded in a non-dispersive medium with the same permittivity. In this section equations in the time domain are derived from which these kernels can be calculated numerically. The basis for the derivations are the Laplace or Fourier transforms of R and T, which are the reflection and transmission coefficients for a finite slab. These quantities are well-known and can be found in elementary books on electrodynamics. The explicit expressions for the Laplace transforms $\hat{R}(s)$ and $\hat{T}(s)$ read

$$\hat{R}(s) = \hat{r}(s) \frac{1 - d^2 \exp(-s\tau) \exp(-\hat{\beta}(s))}{1 - (\hat{r}(s))^2 d^2 \exp(-s\tau) \exp(-\hat{\beta}(s))} \quad (5.1)$$

$$\hat{T}(s) = d \exp(-\hat{\beta}(s)/2) \left(1 - \hat{r}(s) \hat{R}(s) \right) - d, \quad (5.2)$$

where s is the transformed time variable. The function $\hat{r}(s)$ is the reflection coefficient for a semi-infinite slab, i.e.,

$$\hat{r}(s) = \frac{1 - (1 + \hat{\chi}(s)/\varepsilon_r)^{\frac{1}{2}}}{1 + (1 + \hat{\chi}(s)/\varepsilon_r)^{\frac{1}{2}}}. \quad (5.3)$$

The function $\hat{\beta}(s)$ contains the phase information

$$\hat{\beta}(s) = s\tau \left(((1 + \hat{\chi}(s)/\varepsilon_r)^{\frac{1}{2}} - 1 \right) - \frac{\chi(0)\tau}{2\varepsilon_r}. \tag{5.4}$$

By introducing the function $\hat{e}(s)$ as

$$\hat{e}(s) = d \exp(-\hat{\beta}(s)/2) - d, \tag{5.5}$$

the relation between $\hat{R}(s)$ and $\hat{T}(s)$ can be written

$$\hat{T}(s) = \hat{e}(s) - (d + \hat{e}(s))\hat{r}(s)\hat{R}(s). \tag{5.6}$$

The reflection coefficient in Eq. (5.1) may be expanded in a power series as

$$\hat{R}(s) = \hat{r}(s) + \left((\hat{r}(s))^2 - 1 \right) \sum_{i=1}^{\infty} d^{2i} \left(\hat{r}(s) \right)^{2i-1} \exp(-i(\beta(s) + s\tau)). \tag{5.7}$$

Now introduce the functions of time

$$\begin{aligned} r(t) &= \mathcal{L}^{-1} \left\{ \hat{r}(s) \right\} \\ e(t) &= \mathcal{L}^{-1} \left\{ \hat{e}(s) \right\} \\ v(t) &= \mathcal{L}^{-1} \left\{ d^2 \hat{r}(s) \exp(-\hat{\beta}(s)) \right\}, \end{aligned}$$

where $\mathcal{L}^{-1}$ denotes the inverse Laplace transform. A transformation of Eqs. (5.6) and (5.7) to the time domain gives the following expressions for reflection kernel $R(t)$ and the transmission kernel $T(t)$:

$$R(t) = r(t) + \textstyle\sum_{i=0}^{\infty} \mathcal{S}((i+1)\tau) \left[(r * r * v - v)(*r * v)^i \right](t) \tag{5.8}$$

$$T(t) = e(t) - d \left[r * R \right](t) - \left[e * r * R \right](t). \tag{5.9}$$

Furthermore $v(t)$ is related to $e(t)$ by the equation

$$v(t) = \left[r * e * e \right](t) + 2d \left[r * e \right](t) + d^2 r(t). \tag{5.10}$$

Thus $R(t)$ and $T(t)$ are known if the two functions $r(t)$ and $e(t)$ are known.

It will now be seen that the functions $r(t)$ and $e(t)$ satisfy Volterra equations of the second kind. The equation for $r(t)$ is obtained from Eq. (5.3) which can be rewritten as

$$4\varepsilon_r \hat{r}(s) + \hat{G}(s) \left((\hat{r}(s))^2 + 2\hat{r}(s) + 1 \right) = 0.$$

The inverse Laplace transform of this equation is

$$4\varepsilon_r r(t) + \chi(t) + \left[\chi * (2r + r * r) \right](t) = 0, \qquad t > 0. \tag{5.11}$$

The Volterra equation for $e(t)$ is obtained by differentiation of Eq. (5.5) with respect to the transformed time s, giving

$$2\partial_s \hat{e}(s) = -(\partial_s \hat{\beta}(s)) d \exp(-\hat{\beta}(s)/2).$$

The inverse Laplace transform of this equation is the Volterra equation

$$2e(t) + \frac{1}{t}\left[f * e\right](t) + b(t) = 0, \tag{5.12}$$

where

$$b(t) = \mathcal{L}^{-1}\left\{\hat{\beta}(s)\right\} = \frac{\tau}{2\varepsilon_r}\left([\chi' * r](t) + \chi(0)r(t) + \chi'(t)\right) \tag{5.13}$$
$$f(t) = tb(t).$$

Since the equations for $r(t)$ and $e(t)$ both are Volterra equations of the second kind they are well posed and straightforward to solve numerically. At this stage all equations needed for the solution of the direct and inverse scattering problems have been derived. Before turning to the numerical solution of the scattering problems it is worthwhile to comment upon the discontinuities of the scattering kernels.

6 Discontinuities and initial values

The initial values and discontinuities of the scattering kernels are straightforward to obtain from the equations in the previous sections. The initial condition of the reflection kernels r, R, R_b and R_f are obtained from Eqs. (5.11), (4.6), and (4.11), respectively. The values are

$$r(0) = R(0) = R_b(0) = -\frac{\chi(0)}{4\varepsilon_r} \tag{6.1}$$

$$R_f(0) = \frac{\chi(0)}{4\varepsilon_r}(r_0^2 - 1). \tag{6.2}$$

The initial value for T follows from Eqs. (5.9), (5.12), and (5.13) and the initial values for T_b and T_f follow from Eqs. (4.8) and (4.15), respectively

$$T(0) = e(0) = \frac{\tau}{4\varepsilon_r}\left(\frac{\chi(0)^2}{4\varepsilon_r} - \chi'(0)\right) \tag{6.3}$$

$$T_b(0) = t_1 T(0) + r_1 t_1 d R(0) \tag{6.4}$$

$$T_f(0) = t_0 T_b(0) - d t_0 t_1 r_0 R_b(0). \tag{6.5}$$

It is seen that both $r(t)$ and $T(t)$ are continuous functions for positive times whereas the other kernels have discontinuities. The discontinuities only appear at multiples of roundtrips. The following expression for a discontinuity at the time $t = j\tau$ is used in the rest of the paper:

$$[F(j\tau)] = F(j\tau^+) - F(j\tau^-).$$

From Eq. (5.8) it is seen that the reflection kernel $R(t)$ only has one discontinuity occuring at one round trip.

$$[R(\tau)] = -d^2 r(0) = d^2 \frac{\chi(0)}{4\varepsilon_r}.$$

The reflection kernel for the slab with an impedance mismatched backwall, R_b, is discontinuous at the first and the second round trip. The discontinuities follow from Eq. (4.6)

$$[R_b(\tau)] = [R(\tau)] + r_1^2 d^2 R(0) + 2r_1 dT(0)$$
$$[R_b(2\tau)] = r_1^2 d^2 [R(\tau)] .$$

The reflection kernel for the entire slab, R_f, is discontinuous at every roundtrip, due to the impedance mismatched front and back walls. From the Volterra equation for R_f, Eq. (4.11), it is seen that the values of these discontinuities are

$$[R_f(\tau)] = (1 - r_0^2) [R_b(\tau)] - r_0 r_1 d^2 R_f(0) - r_0 a_1 R_b(0)$$
$$[R_f(2\tau)] = (1 - r_0^2) [R_b(2\tau)] - r_0 r_1 d^2 [R_f(\tau)] -$$
$$-r_0 a_1 [R_b(\tau)] - r_0 a_2 R_b(0)$$
$$[R_f(j\tau)] = r_0^2 d^2 [R_f((j-1)\tau)] - r_0 a_{j-2} [R_b(2\tau)] -$$
$$-r_0 a_{j-1} [R_b(\tau)] - r_0 a_j R_b(0), \qquad j = 3, 4, ...$$

As seen from Eq. (4.8) the transmission kernel for the slab with an impedance matched backwall has only a discontinuity at one roundtrip where

$$[T_b(\tau)] = r_1 t_1 d [R(\tau)] = r_1 t_1 d^3 \frac{\chi(0)}{4\varepsilon_r}.$$

The transmission kernel for the entire slab, T_f, is discontinuous at each roundtrip. The values of these discontinuities are obtained from Eq. (4.15) and read

$$[T_f(\tau)] = r_1 d [R_f(\tau)] + t_0 [T_b(\tau)] + r_1 t_1^{-1} a_1 T_b(0)$$
$$[T_f(j\tau)] = r_1 d [R_f(j\tau)] + r_1 t_1^{-1} (a_{j-1} [T_b(\tau)] + a_j T_b(0)), \qquad j = 2, 3, ...$$

7 The direct scattering problem

The direct scattering problem is to determine the scattering kernels R_f and T_f given the susceptibilty kernel $\chi(t)$, the permittivities ε_r and ε_{r1} and the length L of the slab. The numerical tools needed to solve the direct problem boil down to a routine for convolution and a numerical solver of Volterra equations of the second kind. Both of these routines are very simple and they only require a few lines of code. The algorithm to obtain the reflection and transmission kernels R_f and T_f is

1. Solve Eq. (5.11) for $r(t)$.
2. Solve Eqs. (5.13), (5.12), and (5.10) for $b(t)$, $e(t)$, and $v(t)$.
3. Construct $R(t)$ and $T(t)$ from Eqs. (5.8) and (5.9).
4. Solve Eqs. (4.6) and (4.8) for $R_b(t)$ and $T_b(t)$.
5. Solve Eqs. (4.11) and (4.14) for $R_f(t)$ and $T_f(t)$.

In the last step Eq. (4.15) can be used instead of Eq. (4.14) to obtain T_f.

8 The inverse problem

In the inverse problem the kernels R_f and T_f are assumed to be known from experiments and the task is to construct the susceptibility kernel from one of these kernels. The permittivity of the slab, ε_r, and of the surrounding media are also assumed to be known from experiments. In a reflection experiment the permittivity of the slab is obtained from the reflection coefficient r_0 which in turn is determined from the directly reflected pulse $r_0 E^i(0,t)$ in Eq. (4.9). In a transmission experiment the permittivity of the slab is determined from the travel time $L/c = L(\mu_0\varepsilon_0\varepsilon_r)^{1/2}$ of the wavefront. Furthermore the initial value of the susceptibility kernel, $\chi(0)$, is obtained from the attenuation of the directly transmitted pulse, d, in a transmission experiment.

If the reflection kernel, R_f, is known up to a certain time, the susceptibility kernel will be obtained up to the same time from the following scheme:

1. The first roundtrip, i.e. $t < \tau$.
   (a) Solve for $R_b(t) = R(t) = r(t)$ from Eq. (4.11).
   (b) Solve for $\chi(t)$ from Eq. (5.11).
2. The second roundtrip, $\tau < t < 2\tau$.
   (a) Solve for $T(t)$ for $t < \tau$ from Eq. (5.9).
   (b) Solve for $R_b(t)$ for $\tau < t < 2\tau$ from Eq. (4.11).
   (c) Solve for $R(t)$ for $\tau < t < 2\tau$ from Eq. (4.6).
   (d) Solve for $r(t)$ for $\tau < t < 2\tau$ from Eq. (5.8)
   (e) Solve for $\chi(t)$ for $\tau < t < 2\tau$ from Eq. (5.11).

To obtain χ for more than one roundtrip the steps 2(a)-(e) are performed for every new roundtrip.

The inversion of transmission data is not as straightforward as the one for reflection data. The scheme for the inversion is based upon the observation that in the discretized form of the equations that relate the kernel T_f to the susceptibility kernel χ there is a linear mapping from $\chi'(t)$ to $T_f(t)$. Thus if time is discretized with stepsize Δt, the relation between T_f and the time derivative of the susceptibilty kernel, χ' at time $j\Delta t$, where j is an integer, can be written as

$$T_f(j\Delta t) = A_j + B\chi'(j\Delta t). \tag{8.1}$$

The coefficient B is independent of the index j and the coefficient A_j is independent of $\chi'(j\Delta t)$ but is dependent of χ at earlier timesteps. The linear mapping is a consequence of the fact that the only operations that are involved in the equations are convolutions and additions. The initial value $\chi'(0)$ is determined by the initial values in Eqs. (6.1)-(6.5) since $\chi(0)$ is considered to be known. The coefficients A_j and B can be obtained from the discretized version of the equations that determines the reflection kernel T_f. The expressions are however quite lengthy and it is

preferable to obtain the coefficients in the following manner. First A_1 and B are determined. Choose two different dummy values χ_0' and χ_1' of $\chi'(\Delta t)$ and solve the direct problem for the corresponding values of the transmission kernel. If these values of the transmission kernels are denoted T_{f0} and T_{f1}, the following two equations are obtained from Eq. (8.1):

$$T_{f0} = A_1 + B\chi_0'$$
$$T_{f1} = A_1 + B\chi_1'.$$

From this system of equations the coefficients A_1 and B are solved. The value of $\chi'(\Delta t)$ is then obtained from Eq. (8.1). Next the coefficients A_j and the values of $\chi'(j\Delta t)$ are determined for $j > 1$. Assume that $\chi'(t)$ has been determined for all discretized times up to $(j-1)\Delta t$ and is to be determined for $j\Delta t$. Choose a dummy value χ_j' of $\chi'(j\Delta t)$ and solve the direct problem for the the corresponding value, T_{fj}, of the transmission kernel. If this value is denoted T_{fj} it is seen that

$$A_j = T_{fj} - B\chi_j'.$$

The value of $\chi'(j\Delta t)$ is then obtained from Eq. (8.1), i.e.,

$$\chi'(j\Delta t) = (T_f(j\Delta t) - A_j)/B$$

It turns out that the values of A_j are very insencitive of the choosen values χ_j', as expected. Since the initial value, $\chi(0)$, is known the susceptibilty kernel is obtained by numerically integrating $\chi'(t)$ in time.

9 Numerical examples

Three different numerical examples are presented in this section. The first two examples concern the determination of the scattering kernels R_f and T_f and the reconstruction of the susceptibility kernel using these kernels as scattering data. In the third example measured transmitted data is used to obtain the susceptibilty kernel. The trapezoidal rule was used for the discretization of the equations which implies quadratic convergence of the numerical calculations. The direct and inverse algorithms and codes have been checked by comparisons with two other methods, the invariant imbedding method, *cf.* [1] and the Green functions approach, *cf.* [10]. In both cases the agreement was excellent.

The two most common models for dispersion are the Lorentz model and the Debye model. The susceptibility kernel in the Lorentz model reads, *cf.* [8] and [2],

$$\chi(t) = \omega_p^2 \frac{\sin \nu_0 t}{\nu_0} e^{-\nu t/2}, \tag{9.1}$$

where ω_p is the plasma frequency, ν is the collision frequency for the electrons and $\nu_0^2 = \omega_0^2 - \nu^2/4$ where ω_0 is the resonant frequency for the electron bound to the atom. The model is relevant in the optical regime for solids. In the microwave regime solid

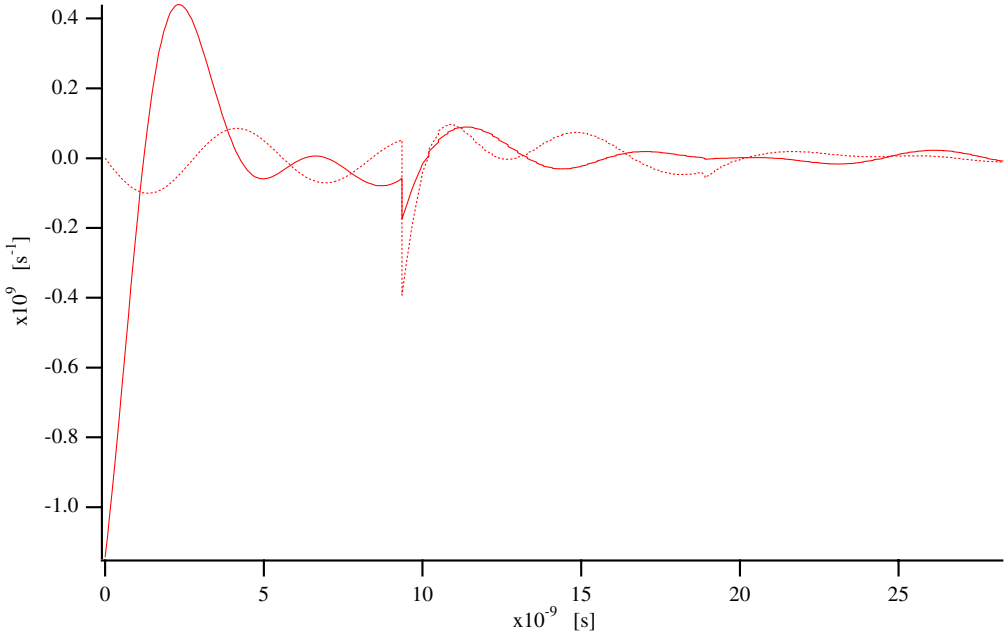

Figure 1: The reflection (dotted line) and transmission kernel (solid line) for a Lorentz medium of length 1 m and with $\omega_p = 10^9$ rad/s, $\omega_0 = 10^9$ rad/s and $\nu = 10^8$ Hz, *cf.* Eq. (9.1). The susceptibility kernel is given in Figure 2.

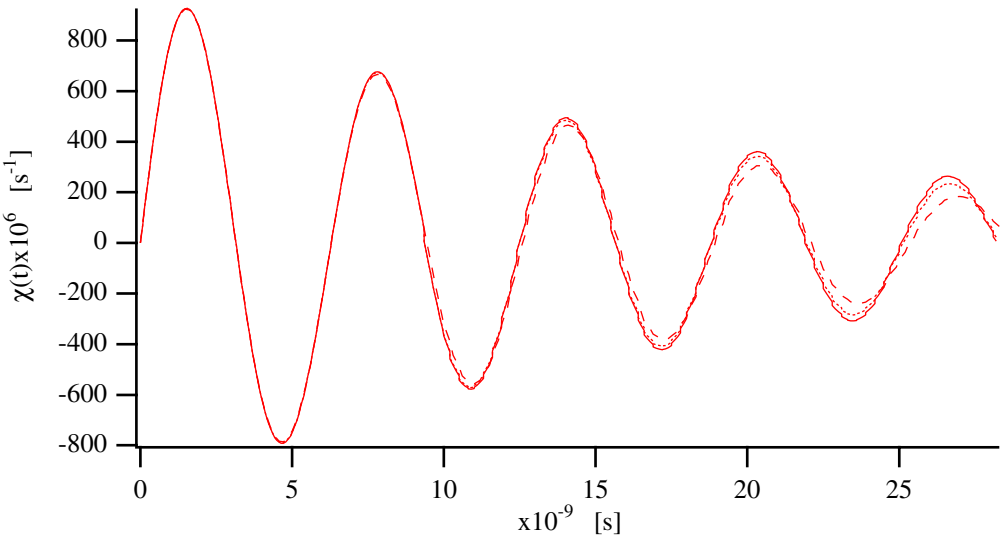

Figure 2: The Lorentz susceptibilty kernel with $\omega_p = 10^9$ rad/s, $\omega_0 = 10^9$ rad/s and $\nu = 10^8$ Hz (solid line). The susceptibility kernels reconstructed from the transmission kernel in Figure 1 using 64 points per roundtrip (dashed line) and 128 points/roundtrip (dotted line).

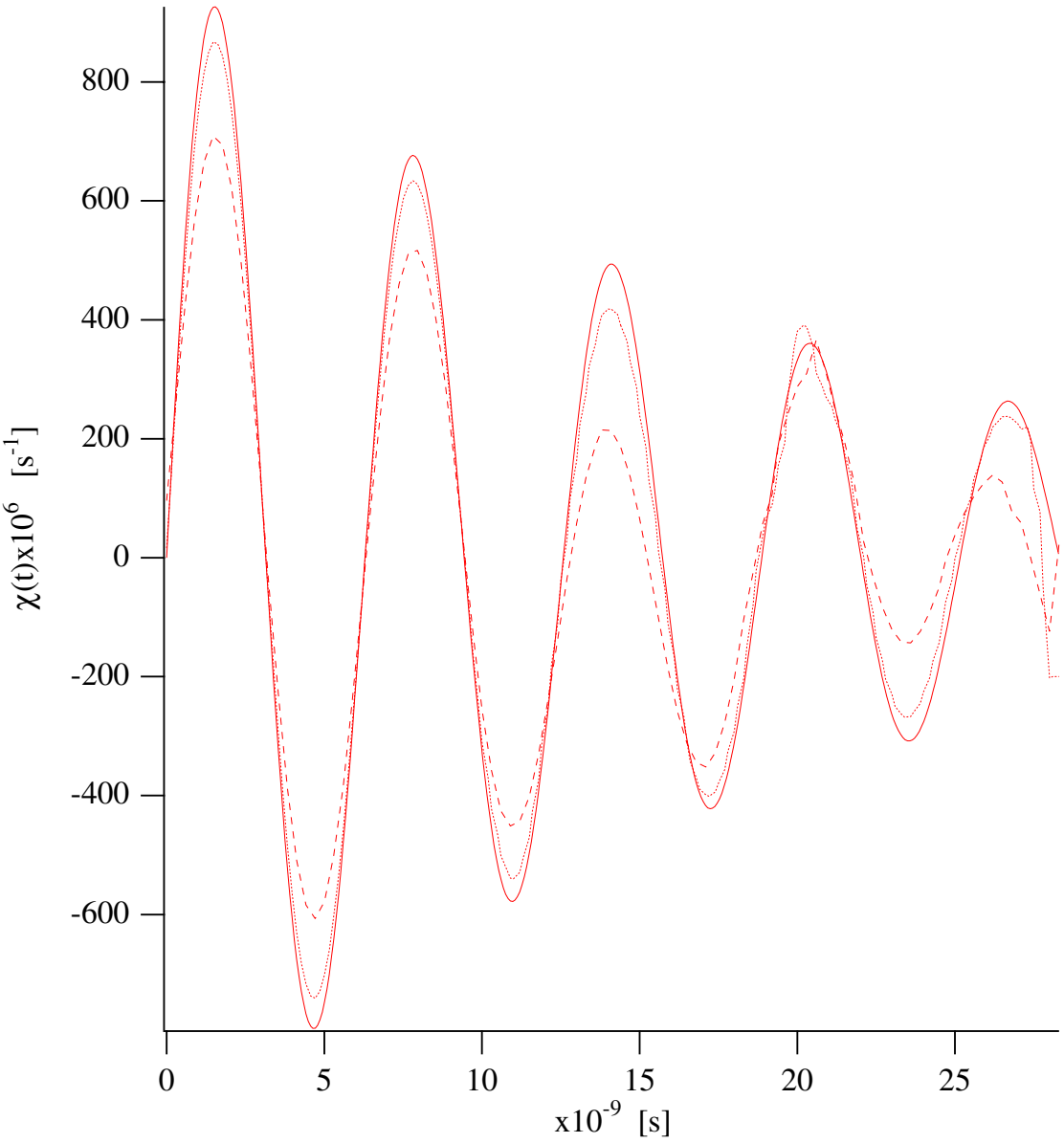

Figure 3: The Lorentz susceptibilty kernel with $\omega_p = 10^9$ rad/s, $\omega_0 = 10^9$ rad/s and $\nu = 10^8$ Hz (solid line). The susceptibility kernels reconstructed from the reflection kernel in Figure 1 using 32 points per roundtrip (dashed line) and 64 points/roundtrip (dotted line).

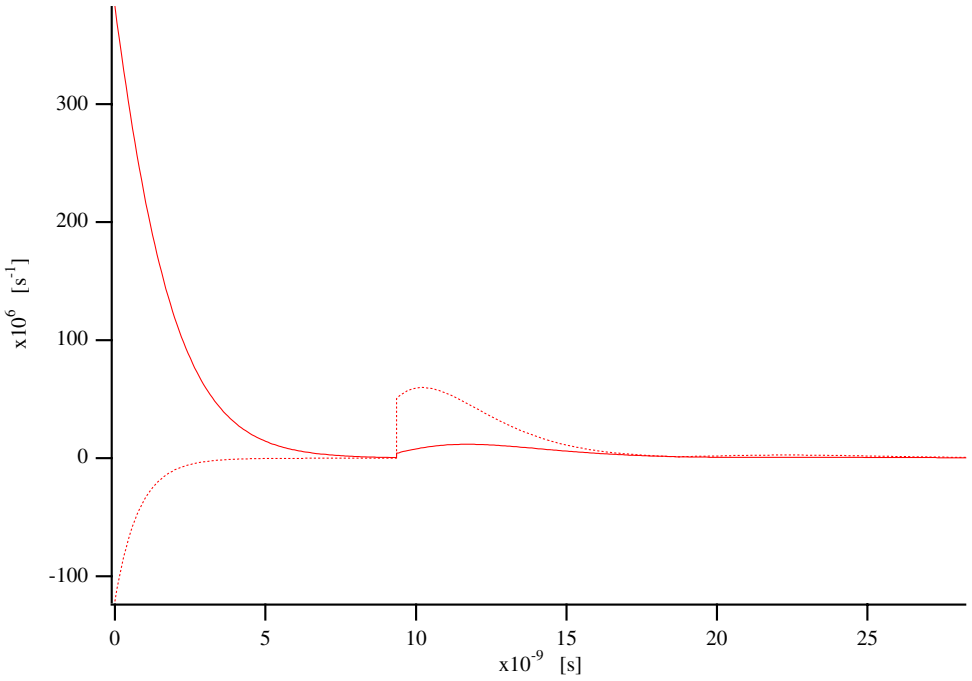

Figure 4: The reflection (dotted line) and transmission kernel (solid line) for a Debye medium of length 1 m and with $\alpha = 10^{10}\,\mathrm{s}^{-1}$ and $\tau = 10^{-9}\,\mathrm{s}$, *cf.* Eq. (9.2). The susceptibility kernel is given in Figure 5.

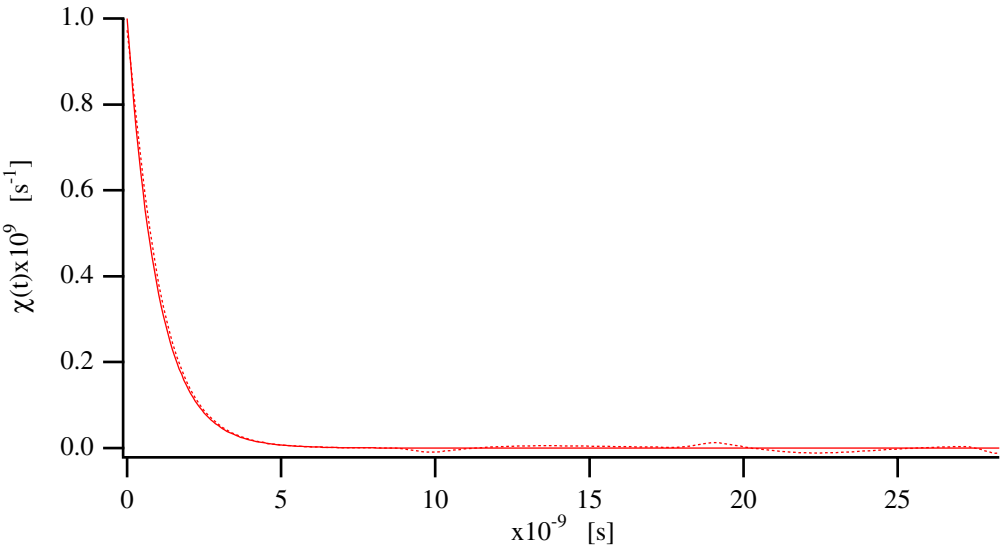

Figure 5: The Debye susceptibilty kernel with $\alpha = 10^{10}\,\mathrm{s}^{-1}$ and $\tau = 10^{-9}\,\mathrm{s}$ (solid line). The susceptibility kernels reconstructed from the reflection kernel of a slab of length 1 m using 64 points per roundtrip (dotted line).

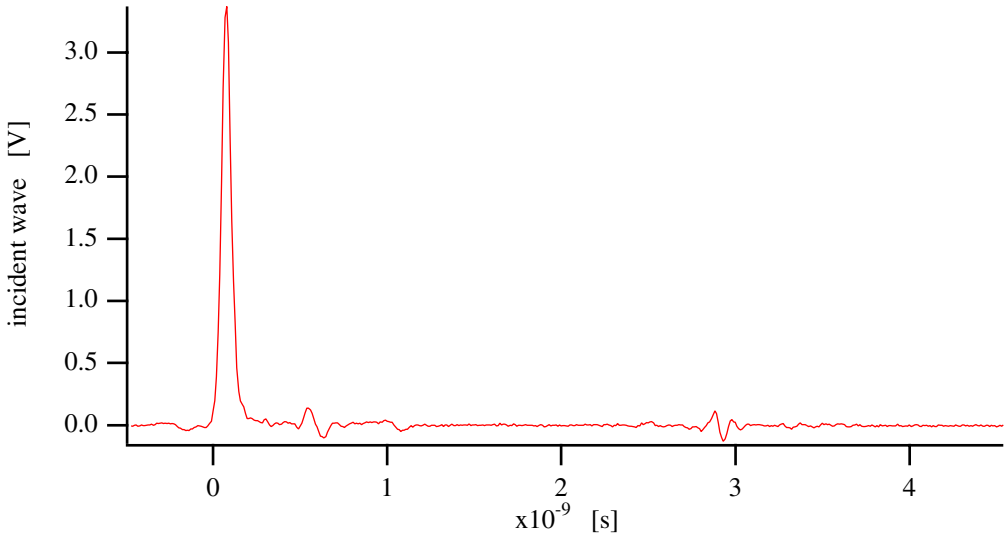

Figure 6: The incident pulse for the open wave-guide experiment.

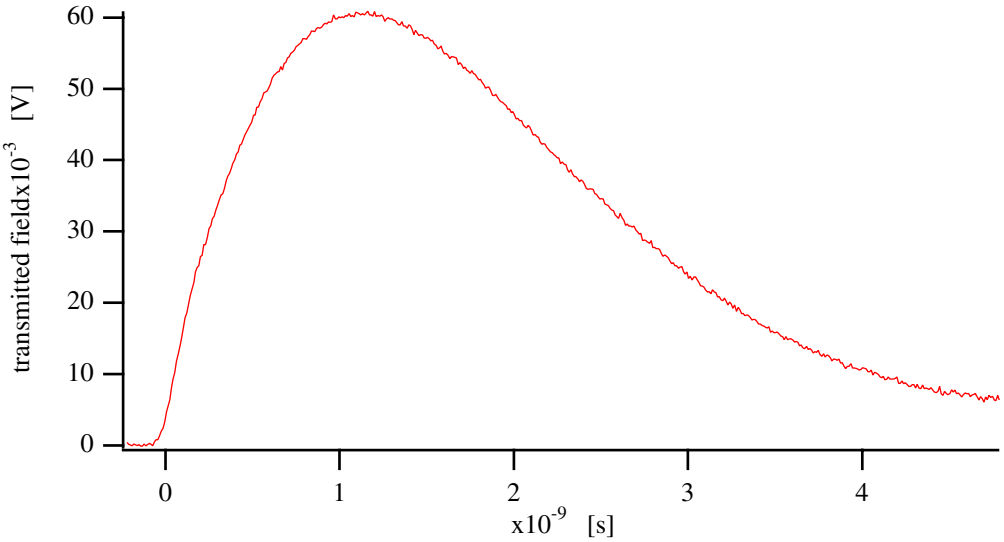

Figure 7: The transmitted pulse for the open wave-guide experiment.

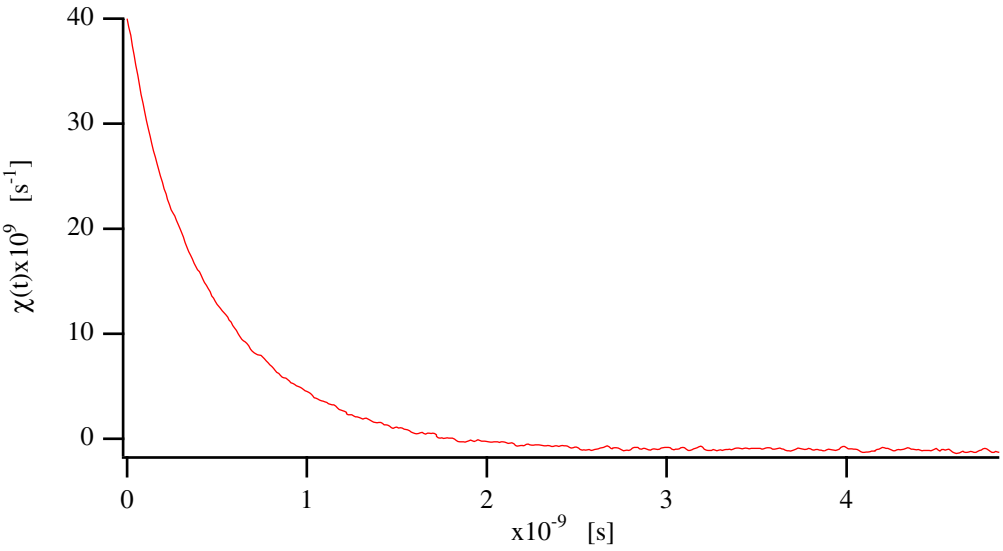

Figure 8: The susceptibility kernel for butanol obtained from the transmission kernel deconvolved from the transmitted field in Figure 6.

materials are approximated by non-dispersive dielectrics and the Lorentz model is superflous. There are however media where dispersive models of Lorentz type are relevant in the microwave regime, eg. gyrotropic media. The Debye model is characterized by the susceptibility kernel, *cf.* [2],

$$\chi(t) = \alpha e^{-t/\tau}. \tag{9.2}$$

The Debye model is appropriate for polar liquids. If an electric field is applied to a polar liquid the liquid will be polarized due to the permanent dipole moments of the molecules. When the electric field is shut off the polarization will decrease exponentially due to the motion and collisions of the molecules. Values of the relaxation time τ for polar liquids at room temperature ranges from ten picoseconds up to one nanosecond , *cf. e.g.*, [7]. Thus microwaves are suitable for the examination of these media.

In the first example a Lorentz model is used. The values of the parameters in the model are $\omega_p = \omega_0 = 10^9$ rad/s and $\nu = 10^8$ Hz. The relative permittivity of the medium is $\varepsilon_r = 2$ and outside the slab there is vacuum, i.e., $\varepsilon_r = 1$. These values are chosen to give a reasonable test of the algorithms rather than to be physically relevant. The length of the medium is one meter and the time trace corresponds to three roundtrips in the slab. The reflection and transmission kernels are shown in Figure 1. Notice the discontinuities of the kernels at one and two roundtrips. The reconstruction of the susceptibility kernel from the transmission kernel is depicted in Figure 2 and from the reflection kernel in Figure 3.

In the second example the slab is one meter long and consists of a Debye medium with $\alpha = 10^{10}\mathrm{s}^{-1}$, $\tau = 10^{-9}$ s and relative permittivity $\varepsilon_r = 2$. The reflection and transmission kernels are depicted in Figure 4 and the reconstructed susceptibility

kernel from the reflection kernel using 64 points per roundtrip is shown in Figure 5. The time trace is three roundtrips. With 128 points per roundtrip the reconstruction is indistinguishable from the true kernel.

In the last example measured data is used. The medium is 1-buthanol which is a typical Debye medium. Buthanol has a relatively long relaxation time (five nanoseconds) which makes it suitable as a reference medium. The complex susceptibility, i.e., the Fourier transform of the susceptibility kernel, can be found in the literature from frequency domain methods for frequencies up to 10 GHz, *cf.* [6], [3] and [4]. The measurement was made for a 20 cm long sample of buthanol. The incident pulse was a 50 ps short pulse *cf.* Figure 6. The transmitted pulse was recorded for 4,8 ns which corresponds to two roundtrips, *cf.* Figure 7. A first order approximation of the transmission kernel was obtained by simply dividing the transmitted pulse by the area of the incident pulse. Of course the transmission kernel then is wrong for the first 50 ps. However, even with this poor deconvolution method the susceptibility kernel comes out surprisingly good and the reconstructed susceptibility kernel agrees well with data found in the literature. There is a high frequency ripple which is the result of the poor quality of the transmission kernel for the first 50 ps. In order to get a smoother curve for the susceptibility kernel the first 50 ps of the transmission kernel was obtained by extrapolation from the rest of the curve. The corresponding reconstruction of the susceptibility kernel is given in Figure 8. The curve fits very well to a Debye model with $\alpha = 4 \cdot 10^{10}\,\mathrm{s}^{-1}$ and $\tau = 0,5$ ns. The relative permittivity was obtained from the time delay of the transmitted wavefront. The value was $\varepsilon_r = 3,3$. The value of $\chi(0)$ can be obtained by measuring the attenuation of the directly transmitted pulse. The attenuation in a 20 cm long sample is too large for the directly transmitted pulse to be seen. If a shorter sample holder is used a rough estimate of $\chi(0)$ can be made. It turns out that it is not crucial for the reconstruction to know the exact value. Even if a value of $\chi(0)$ that is way off is put into the algorithm the reconstructed curve will already after 30-50 ps connect to the true curve. The reconstruction is also insensitive to errors of several percent in the value of ε_r.

10 Conclusions

In the present paper a time domain method for direct and inverse scattering from dispersive media is presented. It is seen that the analysis leads to algorithms for the direct and inverse problems. Numerically these algorithms are very robust and this is expected since all of the equations involved in the solution are Volterra equations of the second kind. The ill-posedness that is present in these kind of inverse problems is localized to the deconvolution of the transmission or reflection kernel from the transmitted or reflected field.

An encouraging result is the reconstruction of a susceptibility kernel from measured data. The result presented in this paper was the very first experiment that was performed in a recently started project on the determination of susceptibilty kernels for dispersive media. By combining the results obtained from reflection and

transmission experiments and also by using different lengths of sample holders it is expected that very good reconstructions of the susceptibility kernels can be obtained. The results can also be further improved by using better deconvolution methods. If pulse generators that can produce pulses of widths less than 10 ps will be available, one would be able to determine the susceptibility kernels for all polar liquids. With the present pulse generators the susceptibility kernels can only be determined with good accuracy for polar liquids with reasonably large relaxation times.

Acknowledgements

Some of the programs for the data processing were written by A. Lundgren and these have been of great help for us. The partial support of the Swedish Research Council for Engineering Sciences is also gratefully acknowledged.

References

[1] Beezley, R. S. and R. J. Krueger, An electromagnetic inverse problem for dispersive media,
J. Math. Phys. N. Y., 26, 317-325, 1985.

[2] Bohren C. F. and Huffman D. R., *Absorption and Scattering of Light by Small Particles*,
(Wiley, New York, 1983).

[3] Cole R. H., "Evaluation of dielectric behaviour by time domain spectroscopy. 1. Dielectric response by real time analysis,"
J. of Phys. Chem., **14**, 1460-1469, 1975.

[4] Cole R. H., "Evaluation of dielectric behaviour by time domain spectroscopy. 2. Complex permittivity,"
J. of Phys. Chem., **14**, 1469-1474, 1975.

[5] Cole R. H., "Time domain reflectometry,"
Ann. Rev. Phys. Chem. **28**, 283-300, 1977 1977,

[6] B. Gestblom and E. Noreland, "Transmission methods in dielectric time domain spectroscopy,"
J. of Phys. Chem., **8**, 782-788, 1977.

[7] Hill N. E. et al, *Dielectric properties and molecular behaviour,*
(Van Nostrand Reinhold, London, 1969).

[8] Jackson J.D., *Classical Electrodynamics*,
(Wiley, New York 1975).

[9] Karlsson A. and Kristensson G., Constitutive relations, dissipation and reciprocity for the Maxwell equations in the time domain,
J. Electro. Waves Applic., **6**, 537-551, 1992.

[10] Kristensson G., "Direct and inverse scattering problems in dispersive media–Green's functions and invariant imbedding techniques,"
In Kleinman R., Kress R., and Martensen E.,editors, *Direct and Inverse Boundary Value problems*, Methoden und Verfahren der Mathematischen Physik, Band 37, pp 105–119, Mathematisches Forschungsinstitut Oberwolfach, FRG, 1989.

[11] Krueger R. J. and Ochs R. L., "A Green's function approach to the determination of internal fields,"
Wave Motion, **11**, 525-543, 1989.

[12] Redheffer R., "On the relation of transmission-line theory to scattering and transfer,"
J. Math. and Phys., **41**, 1-41, 1962.